Spatio-temporal complexity in the clusters generated by fractional Brownian paths

Anna Carbone[a] and H. Eugene Stanley[b]

[a]Physics Department and National Institute of Matter Physics (INFM),
Politecnico di Torino, Corso Duca degli Abruzzi 24, I-10129 Torino, Italy;
[b]Center for Polymer Studies and Department of Physics
Boston University, Boston, Massachusetts 02215, USA

ABSTRACT

The fractal properties of the clusters $\mathcal{C}$ corresponding to the regions whose contour is a fractional brownian path $y(i)$, with Hurst exponent H, and the function $\widetilde{y}_n(i) \equiv (1/n)\sum_{k=0}^{n-1} y(i-k)$, i.e. the moving average of $y(i)$ with window n, have been extensively investigated. The clusters $\mathcal{C}$ form a stationary sequence, which has been characterized by analyzing the *length* ℓ, the *lifetime* τ and the *area* s of the single cluster. The *length* and the *area* are related to the *duration* by : $\ell \sim \tau^{\psi_\ell}$ and $s \sim \tau^{\psi_s}$, where $\psi_\ell = 1$ and $\psi_s = 1 + H$. Moreover, we have found that $P(\ell) \sim \ell^{-\alpha}$, $P(\tau) \sim \tau^{-\beta}$ and $P(s) \sim s^{-\gamma}$, with $\alpha = \beta = 2 - H$ and $\gamma = 2/(1+H)$. This means that the probability distribution functions of ℓ, τ, and s are power-law with exponents depending on H. Furthermore, the rich fractal structure of the patterns $\mathcal{C}$ has allowed to determine the time dependent Hurst exponent with great accuracy. We have also demonstrated that the cluster *area*, *length* and *lifetime* exhibit the characteristic scaling behavior of systems evolving through self-organized critical states.

Keywords: Fractional Brownian path, Systems obeying scaling laws, Complex systems, Self-organized criticality

1. INTRODUCTION

Fractional Brownian processes have been proposed as a mathematical model for a wide diversity of stochastic phenomena occurring in real extended physical systems exhibiting different degrees of correlation. The variance at large t scales as a power law,

$$\sigma^2 \sim t^{2H} \quad , \tag{1}$$

where H is the Hurst exponent, ranging from 0 to 1. The value $H = 0.5$ corresponds to the ordinary uncorrelated Brownian motion, while $H < 0.5$ and $H > 0.5$ correspond respectively to anticorrelated and correlated signals. The analysis of the Hurst exponent is nowadays considered a practical instrument in fields as biophysics (DNA sequence, gait fluctuations), econophysics, cloud breaking and many others.[1–21] For example, one can discriminate heartbeat intervals of healthy and sick hearts on the basis of the value of H. Stock price volatility shows a degree of persistence ($0.7 < H < 0.8$) larger than that of the return series ($H \sim 0.5$), a fact which is exploited when practical investment tools have to be developed. The validation of climate models is based on the analysis of long-term correlation of atmospheric series.

In order for the above mentioned classifications to be reliable, several techniques have been thus proposed with the main purpose to extract as accurate as possible values of the Hurst exponent from the data set. Among the number of different techniques that have been proposed to estimate the correlation exponent of fractal stochastic signals we only mention the spectral analysis, the correlograms and semivariograms, the rescaled range analysis, the Fano factor, the Allan variance, the Detrended Fluctuation Analysis and very recently the Detrended Moving Average analysis. These techniques calculate appropriate statistical functions over the signal in the time or in the frequency domain. We will briefly review here only the *Rescaled Range Analysis* and the *Detrending Fluctuation Analysis* that can be considered as precursors of the *Detrending Moving Average Analysis*.

E-mail: anna.carbone@polito.it; hes@bu.edu

Noise in Complex Systems and Stochastic Dynamics II, edited by Zoltán Gingl, José M. Sancho, Lutz Schimansky-Geier, Janos Kertesz, Proc. of SPIE Vol. 5471 (SPIE, Bellingham, WA, 2004) · 0277-786X/04/$15 · doi: 10.1117/12.548618

2. DETRENDING MOVING AVERAGE ALGORITHM

The *Rescaled Range Analysis* (R/S), was proposed by Hurst and was motivated by a systematic analysis of the records of water discharges from the Lake Albert.[2] The stochastic time series $y(i)$ with $i = 1, 2, ...N_{max}$ is divided into boxes of equal size n. The functions:

$$X_i = \sum_{j=kn+1}^{i} [y(j) - < y >] \tag{2}$$

and

$$S = \sqrt{\frac{1}{n}\sum_{j=1}^{n}[y(j) - < y >]} \tag{3}$$

are calculated in the k_{th} box, $< y >$ represents the average value of the time series $y(i)$ over each box and is given by $1/n \sum_{i=kn+1}^{(k+1)n} y(i)$. The Rescaled Range R/S function is given by:

$$\frac{R}{S} = \frac{1}{S}[max(X_i) - min(X_i)] \ , \tag{4}$$

where the functions $max(X_i)$ and $min(X_i)$ are calculated over the intervals $kn + 1 << i << (k + 1)n$. The function R/S is then averaged over all the boxes of equal size n. By iterating the calculation of R/S for different box amplitudes n, a relationship between R/S and n is obtained,that in the presence of scaling is of power-law type.

The technique named *Detrended Fluctuation Analysis* (DFA) has been developed later. According to the DFA, after dividing the series $y(i)$ in boxes of equal size n, a polynomial fit $y_{\rm pol}(i)$ is calculated in each box.[5, 6, 15, 16] Then, the generalized variance $\sigma_{\rm DFA}$ about the polynomial fit $y_{\rm pol}(i)$

$$\sigma_{\rm DFA} \equiv \sqrt{\frac{1}{N_{\rm max}} \sum_{i=1}^{N_{\rm max}} [y(i) - y_{\rm pol}(i)]^2} \ , \tag{5}$$

is calculated over different size boxes. $N_{\rm max}$ is the length of the series. The relationship $\sigma_{\rm DFA} \propto n^H$ is obtained for long-memory correlated processes. The advantage of the DFA over the R/S method is that it allow to detect the correlation exponent in nonstationary time series avoiding the spurious detection of long-range correlation which are an artifact of nonstationarity.

The *Detrended Moving Average* (DMA) analysis has been recently developed .[9–11] The DMA technique is based on the following function:

$$\sigma_{\rm DMA} \equiv \sqrt{\frac{1}{N_{\rm max} - n} \sum_{i=n}^{N_{\rm max}} [y(i) - \widetilde{y}_n(i)]^2} \ , \tag{6}$$

which is still a generalized variance but now about the function $\widetilde{y}_n(i)$:

$$\widetilde{y}_n(i) \equiv \frac{1}{n} \sum_{k=0}^{n-1} y(i-k) \ . \tag{7}$$

$\widetilde{y}_n(i)$ is the moving average of window size n, i.e. the average of the signal over n points. It is a linear operator, which basically performs a discrete convolution of the signal. The outputs are the low-frequency components of the signal, filtered according to the window amplitude n. The function $\sigma_{\rm DMA}$ shows a power-law dependence on n, i.e. $\sigma_{\rm DMA} \sim n^H$, when the series is long-range correlated.[9–11]

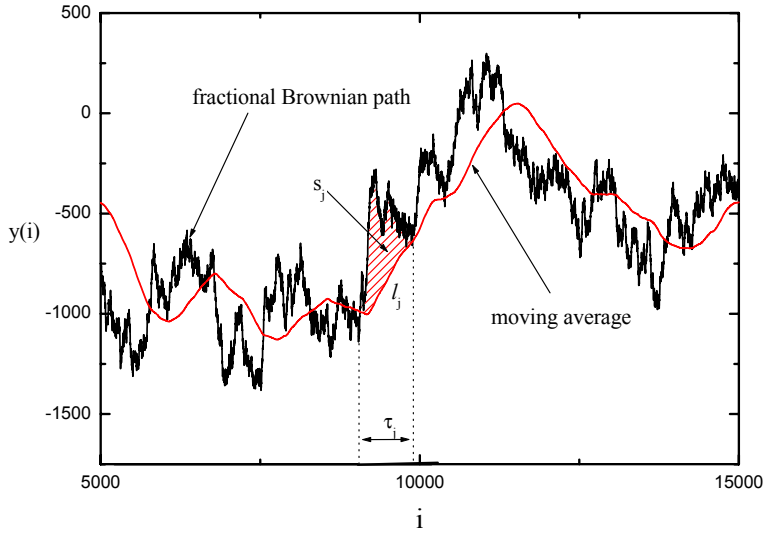

Figure 1. Stochastic series $y(i)$ obtained by the random midpoint displacement algorithm with $H = 0.5$. The moving average $\widetilde{y}_n(i)$ with window $n = 1000$ is also shown. The shaded region represents the area of the cluster. The lifetime and the length of the cluster have been also indicated.

Thanks to the higher accuracy of the moving average filter compared to the polynomial filter, the DMA algorithm exhibit better performances in detrending the nonstationary series. Furthermore, the DMA algorithm requires shorter execution time than the DFA algorithm because in each box n (or equivalently for each moving average window n)(a) it does not need to estimate the coefficients of the polynomial trend and (b) the moving average function is updated at each point by adding the last and discarding the first element of the sequence.

We have also shown that the DMA can be dynamically implemented to get the local scaling properties of non-stationary stochastic series. In this section, we will show how it is possible to determine the local correlation degree of the series (i.e. the dependence of the the Hurst exponent on time) using the DMA algorithm. This task has been fulfilled by local implementation of the DMA algorythm over partially overlapping subsets of the analyzed series. In practice, we apply the DMA algorithm on the ensemble of points obtained by the intersection of the signal with a sliding window W_s of size N_s, moving along the series with step δ_s. The scaling exponent is calculated for each subset according to the procedure described in the previous section. Thus, a sequence of values of the Hurst exponent is obtained. The size of this sequence ranges from 1 (in the trivial case of a unique subset coinciding with the entire series) to $N_{\max} - N_s$ (in the case of a sliding window W_s moving point-by-point along the series: i.e. with $\delta_s^{\min} = 1$). The minimum size $N_s^{\min}$ of each subset is defined by the condition that the scaling law $\sigma_{\mathrm{DFA}} \propto n^H$ holds in the subset (typically $N_s^{\min} = 2000 \div 3000$). The maximum resolution of the technique is achieved with $N_s^{\min}$ and $\delta_s^{\min}$.

First, we have tested the feasibility and the accuracy of the dynamic detrending algorithm on artificial series. Such series have been generated by the random midpoint displacement (RMD) algorithm, which produces signals behaving as fractional Brownian paths with assigned Hurst exponent.[42]

Then, we have applied the DMA algorithm to the log-return of German financial series (tick-by-tick sampled every minute): the DAX (stock market index), the BUND and the BOBL (government bond)[24–36] . If $p(t)$ indicates the price at the time t, the log-return $r(t)$ is

$$r(t) = \log p(t + \Delta t) - \log p(t) \tag{8}$$

Figure 2 shows the log-log plots of the Hurst of the function σ_{DMA} (Eq.(6)) for the returns and for the volatility of the DAX, of the BUND and of the BOBL. It has been found that the Hurst exponent is approximately equal for the three return series (it is equal to 0.49 ± 0.05). Conversely, the Hurst exponent of the volatility series is respectively (a) 0.70 ± 0.05 for the BOBL; (b) 0.72 ± 0.05 for the BUND ; (c) 0.78 ± 0.05 for the DAX.

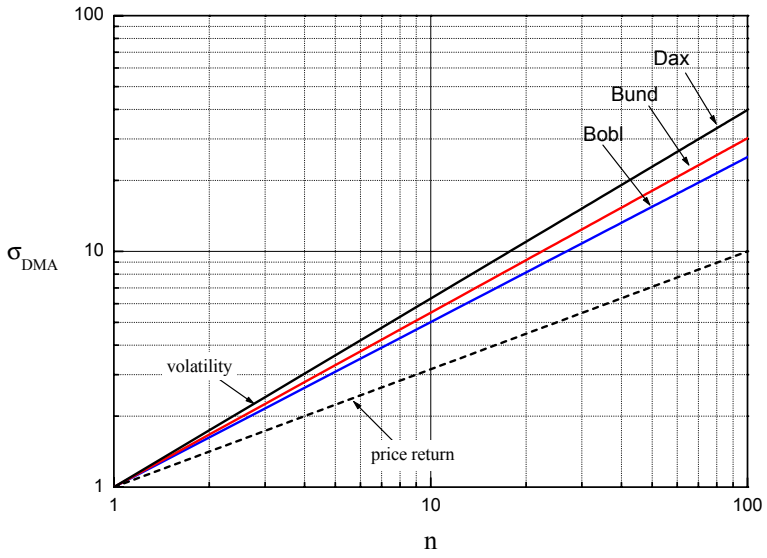

Figure 2. Log-log plots of the function ($\sigma_{\mathrm{DMA}} \propto n^H$ for the return and for the volatility of german financial series (Bobl, Bund, Dax).

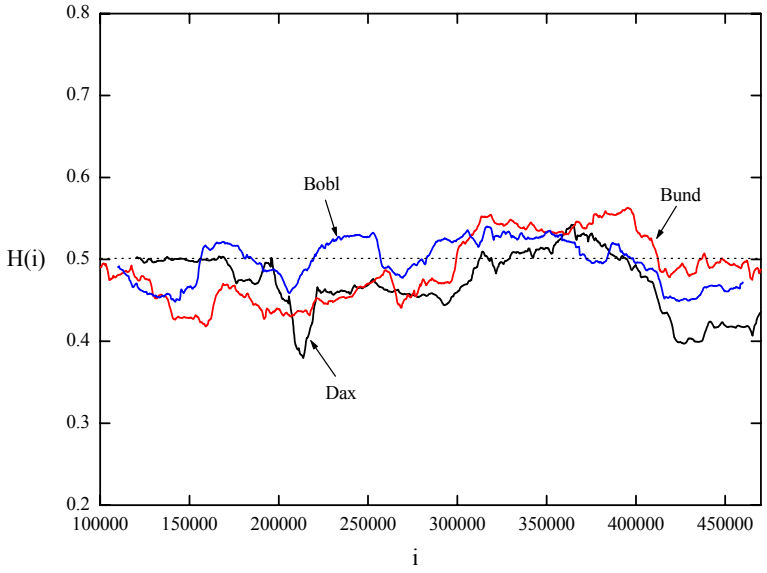

Figure 3. (a) Time-dependent Hurst exponent $H(t)$ for the series of log-returns of the DAX stock index (black), of the BOBL bond index (blue), of the BUND bond index (red).

Figure 3 shows the exponent $H(i)$ for the returns of the DAX, of the BUND and of the BOBL. The size of the subsets is $N_s = 5000$ and the step is $\delta_s = 100$. The parameter n varies from 10 to 1000 with step 2.

It is apparent on comparing Fig. 3(a) with Figs. 3(b) and 3(c) that the artificial series are characterized by a local variability of the correlation exponent weaker than those of the BOBL and DAX series. The small fluctuations exhibited by the $H(i)$ of the artificial series should be considered as the limits of accuracy of the technique. Table (1) shows the means and the standard deviations relative to the average value of the scaling exponents $\alpha(t)$ for the artificial series and for the financial series.

Table 1. Average value of the Hurst exponent H for the log-return and for the volatility respectively for the DAX stock market index, for the BUND and the BOBL government bond. The standard deviation (relative to the mean) of the time dependent Hurst exponent $H(i)$ is reported in the last column. The results provide evidence that a more complex dynamics characterizes the formation of the DAX returns compared to BOBL and BUND bonds, a fact that might be also responsible for the higher value of the Hurst exponent of the volatility of the DAX compared to the BOBL and BUND series.

Series	log-return	volatility	$\Delta H(i)$
DAX	0.49 ± 0.05	0.78 ± 0.05	0.041
BUND	0.49 ± 0.05	0.72 ± 0.05	0.034
BOBL	0.49 ± 0.05	0.70 ± 0.05	0.032

It is interesting to compare the DAX (german stock market index) to the BUND and the BOBL (german governative bond) behaviors. We have found a higher degree of time variability in the DAX than in the Bund and in the BOBL. By comparing the solid curves in Fig. 3, one can notice that the $H(i)$ for the DAX is asymmetric with respect to the reference value $H = 0.5$ (dashed lines). The regions corresponding to anticorrelated values of $H(i)$ (i.e. $H(i) < 0.5$) should be responsible for the clustering effect leading to the stronger long-range positive correlation of the volatility of the DAX compared to the BUND and the BOBL.[31] We have also calculated the Hurst exponent of the absolute value of the return and also of the *square* of the absolute value of the return (that are two possible definitions of the volatility). We found respectively $H = 0.70 \pm 0.05$ and $H = 0.66 \pm 0.05$ for the BOBL series,$H = 0.72 \pm 0.05$ and $H = 0.68 \pm 0.05$ for the BUND series while it is respectively $H = 0.78 \pm 0.05$ and $H = 0.73 \pm 0.05$ for the DAX series. It is well know that the value of the Hurst exponent is slightly dependent on the analytical form of the volatility and on the sampling interval (high-frequency or daily). However, the results obtained by the dynamic detrending moving average algorithm have systematically indicated a strong correlation between the average Hurst exponent H of the volatility and the standard deviation of the time-dependent $H(i)$ of the log-return. Conversely, no correlation seems to exist between $H(i)$ and the average Hurst exponent of the log-return, which, as already discussed, is equal to 0.49 ± 0.05 for all the analyzed financial series. The higher degree of multifractality exhibited by the DAX compared to the BUND and to BOBL series might be related to richer complexity of the stock market index compared to the flatness and stability of the government bond.

3. SCALING LAW OF THE AREA S, LENGTH ℓ AND LIFETIME τ OF THE CLUSTERS

In order to gain a deep insight in the mechanism allowing the function σ_{MA} to capture the scaling properties of long-range correlated signals, we have analyzed the local scaling features of the function $C_n(i)$:

$$C_n(i) = y_n(i) - \widetilde{y}_n(i) \ . \tag{9}$$

$C_n(i)$ generates, for each $\widetilde{y}_n(i)$, a sequence of *clusters* $\mathcal{C}$, corresponding to the areas delimited by $y(i)$ and $\widetilde{y}_n(i)$ between two consecutive intersections(see Fig. 1).

Three measures have been used to characterize each cluster: the *length or the diameter*:

$$\ell_j \equiv \sum_{i=i_c(j)}^{i_c(j+1)} \widetilde{y}_n(i) \ , \tag{10}$$

the *lifetime*:

$$\tau_j \equiv i_c(j+1) - i_c(j) \ , \tag{11}$$

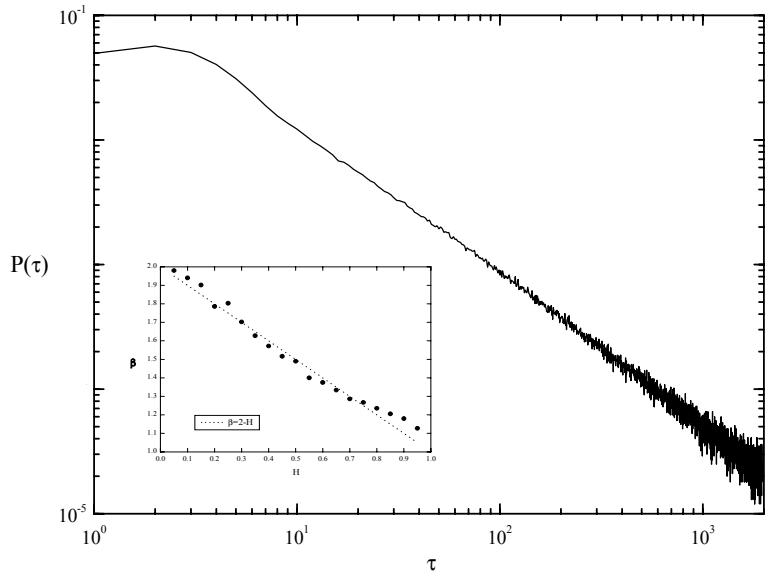

Figure 4. First return probability distribution function $P(\tau)$ of the crossing points between $\widetilde{y}_n(i)$ and $y(i)$. The artificial series has been generated with Hurst exponent $H = 0.5$. The *pdf* is a power-law $P(\tau) \sim \tau^{\beta}$. The saturation at low values of τ is a numerical artifact due to the lack of accuracy for small window n. The inset shows the exponent β obtained for artificially generated series (dots) having different Hurst exponent (ranging from 0.05 to 0.95). The continuous line corresponds to the theoretical values $\beta = 2 - H$.

the area:

$$s_j \equiv \sum_{i=i_c(j)}^{i_c(j+1)} |y(i) - \widetilde{y}_n(i)| \Delta i \quad . \tag{12}$$

In Eqs. (10,11,12), $i_c(j)$ and $i_c(j+1)$ are the values of the index i corresponding to two consecutive intersections between $\widetilde{y}_n(i)$ and $y(i)$ and Δi is the time interval corresponding to the elementary instance of fluctuation.

Let ℓ and s indicate the value of the length and of the area obtained by averaging ℓ_j and s_j over the subset of clusters $\mathcal{C}$ having the same average lifetime τ. The log-log plots of ℓ and s vs. τ have been found to be consistent with linearity over more than two decades, i.e., with the power law relationships

$$\ell \sim \tau^{\psi_\ell} \qquad [\psi_\ell = 1] \ , \tag{13}$$

and

$$s \sim \tau^{\psi_s} \qquad [\psi_s = 1 + H] \ . \tag{14}$$

The probability density function (*pdf*) of the cluster lifetime τ, of the cluster length ℓ and of the cluster area s have been also investigated. The results are consistent with power-law behavior, i.e.:

$$P(\tau) \sim \tau^{-\beta} \quad . \tag{15}$$

$P(\tau)$ is the first return probability distribution of the intersections between $\widetilde{y}_n(i)$ and $y(i)$. Thus, the exponent β can be calculated, it is:

$$\beta = 2 - H \quad . \tag{16}$$

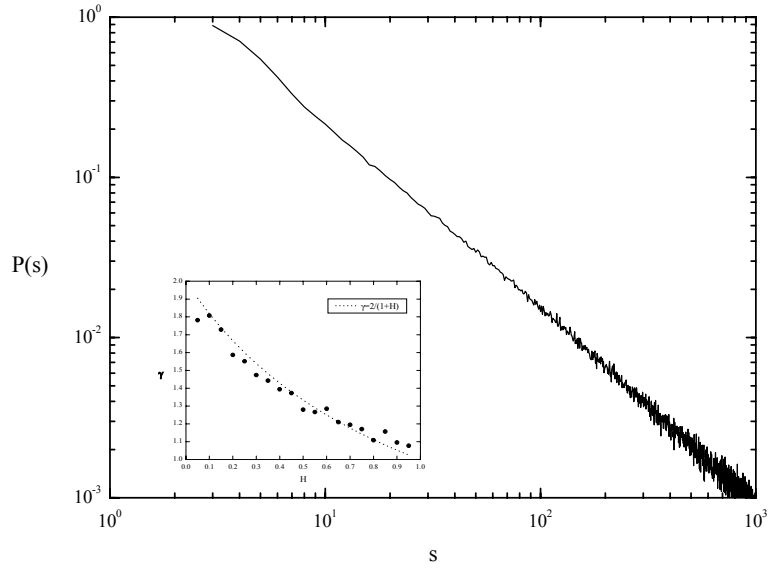

Figure 5. Probability distribution function $P(s)$ of the cluster area s. The artificial series has Hurst exponent $H = 0.5$. The *pdf* shows a linear behavior in log-log scales, consistent with a power law $P(s) \sim s^{\gamma}$. The inset shows the exponent γ obtained for artificially generated series (dots) having different Hurst exponents (ranging from 0.05 to 0.95). The continuous line corresponds to the theoretical values $\gamma = 2/(1+H)$.

Using Eqs. (13) and (14) , the probability density functions $P(\ell)$ and $P(s)$ can be expressed in terms of $P(\tau)$,

$$P(\ell) = P(\tau)\frac{d\tau}{d\ell} \sim \ell^{-\alpha} \tag{17}$$

$$P(s) = P(\tau)\frac{d\tau}{ds} \sim s^{-\gamma} \ . \tag{18}$$

Using Eqs. (13) and (17) and taking into account Eq.(16), the exponent α can be written in terms of β and Hurst exponent as

$$\alpha = \beta \ , \tag{19}$$

and

$$\alpha = 2 - H \ . \tag{20}$$

Analogously, using Eqs. (14) and (18) and taking into account Eq.(16), γ can be expressed in terms of β and ψ_s

$$\gamma = \frac{\beta + 1 - \psi_s}{\psi_s} \ , \tag{21}$$

and in terms of H:

$$\gamma = \frac{2}{1+H} \ . \tag{22}$$

We have calculated the exponents α, β, and γ for a wide range of parameters: $N_{\max}$ ranges from 2^{14} to 2^{21} while n ranges from 2^3 up to 2^{13}. The exponents β and γ are plotted against H in the insets of Figs. 4 and 5, and compared with the theoretical expected values of Eqs. (20) and (28).

4. FINGERPRINTS OF DIRECTED SELF-ORGANIZED CRITICALITY IN THE CLUSTERS $\mathcal{C}$

It is noteworthy that the scaling properties of the $\mathcal{C}$ clusters have the same mathematical strtucture of those proposed within the self-organized criticality (SOC) model .[47–62] In recent years, there has been a huge interest in the study of many variants of the sandpile models mainly because SOC has demonstrated the ability to describe time-space correlated evolution of several critical systems.

Sandpile models are cellular automata (CA) with an integer or continuous variable z_i defined on a d-dimensional lattice of size L . At each time step a particle (or energy) is added to a randomly chosen site, until the variable z_i, which denotes the number of grains (or the energy) at site i reaches the threshold value z_c. When this occurs the site "relaxes," i.e.,

$$z_i \to z_i - z_c \ , \tag{23}$$

and the particles are isotropically transferred to the nearest neighbors

$$z_{i'} \to z_{i'} + y_{i'} \ . \tag{24}$$

The instability of a site can induce a number of other sites to become unstable, because of the particles received, they exceed the threshold. From the moment a site topples, the addition of particles stops until all sites have relaxed ($z_i < z_c$ for all i). This condition assures that the driving force is 'slow' being the driving time exceedingly longer than the characteristic time of toppling instances. The sequence of toppling events during this interval constitutes an avalanche. For conservative models, the number of transferred particles equals the number of particles lost by the relaxing site ($\sum y_j = z_c$) and dissipation occurs only at boundary, from which particles can escape the system. Under these conditions the system reaches a stationary state characterized by a sequence of avalanches. Since the SOC algorithm is implemented basically as a cellular automaton, the cluster growth is intrinsically of diffusive nature.

The total number of toppling sites s, the avalanche diameter l and the lifetime τ are conveniently adopted to characterize the dynamics ruling the avalanche evolution. The quantities s, l and τ are related by power law: $s \sim \tau^{D_s/z}$ and $l \sim \tau^z$, D_s and z respectively being the avalanche size exponent and the dynamical exponent.

The avalanche *pdf's* for s, l and τ scale respectively as:

$$P(s) \sim s^{-\tau_s} f(s/s_c) \ , \tag{25}$$

$$P(l) \sim l^{-\tau_l} f(l/l_c) \ , \tag{26}$$

$$P(\tau) \sim \tau^{-\tau_t} f(\tau/\tau_c) \ . \tag{27}$$

As usual, the quantities s_c, l_c and τ_c are the cut-off values respectively of the area, length and duration.

Using the above set of equations, one obtains the following relationships among the SOC exponents:

$$\tau_t = z\tau_l \ , \tag{28}$$

$$(\tau_t - 1)z = (\tau_s - 1)D_s \ , \tag{29}$$

By comparing the characteristic exponents z, D_s τ_l, τ_t, τ_s with those obtained for the clusters $\mathcal{C}$, it is evident that our system behaves as a self-organised critical system, it is indeed:

$$z = 1 \ , \tag{30}$$

$$D_s = 1 + H \ , \tag{31}$$

$$\tau_l = 2 - H \ , \tag{32}$$

$$\tau_t = 2 - H \ , \tag{33}$$

$$\tau_s = \frac{2}{1+H} \ . \tag{34}$$

It is also worthy of note that the previous exponents, for the case of uncorrelated Brownian motion i.e. the simple random walk with $H = 0.5$, coincide with the exponents of the Dhar-Rawasmany model.

5. CONCLUSION

In summary, the statistical properties of the sequence of stationary self-affine clusters $\mathcal{C}$ generated by the intersections of the time series $y(i)$ with the moving average $\widetilde{y}_n(i)$ have been analyzed. For model series of length up to $N_{\max} = 10^{21}$ we have calculated the *lifetime* τ, the length $\ell \sim \tau^{\psi_\ell}$ and the area $s \sim \tau^{\psi_s}$ and the pdfs $P(\ell) \sim \ell^{-\alpha}$, $P(\tau) \sim \tau^{-\beta}$ and $P(s) \sim s^{-\gamma}$ of the clusters $\mathcal{C}$. Our results are consistent with power laws whose exponents agree with the predictions $\psi_l = 1$, $\psi_s = 1 + H$, $\alpha = \beta = 2 - H$, and $\gamma = 2/(1 + H)$ for a wide range of H $(0.05 < H < 0.95)$.

We have also reported on the *local* scaling exponent $H(i)$ of financial and artificial series. We calculated $H(i)$ using the DMA technique.[9–11, 38] The ability of the DMA technique to perform such analysis relies on the local scaling properties of the function (9). The DMA algorithm allows to calculate the exponent $H(i)$, without any *a priori* assumption on the stochastic process and on the probability distribution function of the random variables entering the process, as in the case of the Kitagawa grid and of the extended Kalmann filtering methods.[44] The proposed technique examines the local scaling around a given instant of time. This is a main advance with respect to the standard wavelet transform or the higher-order power spectrum technique, which instead operate on the global properties of the series by Legendre or Fourier transform of qth-order moments. Our study indicates several directions for future research. Using the dynamic algorithm here presented, or a variant under development, the multifractal properties of long-range correlated nonstationary series can be analyzed locally rather than globally. We have found a stronger variability of the exponent $H(i)$ in financial time compared to monofractal artificial series, consistent with the possibility of a multiscaling mechanism of the price formation.

Finally, we have also shown that the function $C_n(i)$ generates *fractal directed patterns* showing spatio-temporal complexity, arguing that the cluster area, length and duration exhibit the characteristic scaling behavior of SOC clusters. The function $C_n(i)$ acts as a *magnifying lens*, zooming in (or out) the 'avalanches' formed by the cluster construction rule, where the *magnifying power* of the zoom is set by the value of the amplitude window n. On the basis of the construction rule of the clusters $C_n(i) \equiv y(i) - \widetilde{y}_n(i)$ and of the relationship among the exponents, we hypothesize that our model might be considered as a generalized stochastic directed model, including the Dhar-Rawasmany (DR) and the stochastic models as particular cases. As in the DR model, the growth and annihilation of our clusters are obtained from the set of intersections of two random walk paths, and we argue that our model is a variant of the directed self-organized criticality scheme of the DR model.

Acknowledgment

A.C. acknowledges support by the MIUR under the program PRIN2003 *Excess noise in nanoscaled optoelectronic devices.* H.E.S thanks the NSF (grant CHE0096892) and the NIH/National Center for Research Resources (P41RR13622) for support.

REFERENCES

1. J. Feder, *Fractals* (Plenum, New York, 1988), p. 172.
2. H.E.Hurst, R.P. Black and Y.M.Simaika *Long-term storage: An experimental study* (Constable, London, 1965).
3. M.S. Taqqu, V. Teverovsky, and W. Willinger, "Estimators for long-range dependence: an empirical study", Fractals, **3**, pp. 785 (1995)

4. S.V. Buldyrev, A.L. Goldberger, S. Havlin, R.N. Mantegna, M.E. Matsa, C.-K. Peng, M. Simons, and H.E. Stanley, "Long-range correlation properties of coding and noncoding DNA sequences: GenBank analysis", Phys. Rev. E, **51**, Issue 5, pp. 5084-509 (1993)
5. C.-K. Peng, S.V. Buldyrev, A.L. Goldberger, S. Havlin, M. Simons, and H.E. Stanley, "Finite-size effects on long-range correlations: Implications for analyzing DNA sequences", Phys. Rev. E, **47**, pp. 3730-3733 (1993)
6. C.K. Peng, S. V. Buldyrev, S. Havlin, M. Simons, H. E. Stanley, and A. L. Goldberger, "Mosaic organization of DNA nucleotides" Phys. Rev. E **49**, 1685 (1994).
7. P. Gopikrishnan., V. Plerou, L. A. N. Amaral, M. Mayer and H. E. Stanley, "Scaling of the distribution of fluctuations of financial market indices", Phys. Rev. E **60**, Issue 5, pp. 5305-5316 (1999)
8. H. E. Stanley, V. Afanasyev, L.A.N. Amaral, S.V. Buldyrev, A.L. Goldberger, S.Havlin, H. Leschhorn, P. Maass, R.N. Mantegna, C.-K. Peng, P.A. Prince, M.A. Salinger, M.H.R. Stanley, G.M. Viswanathan, "Anomalous fluctuations in the dynamics of complex systems: from DNA and physiology to econophysics", Physica A, **224**, pp. 302-321 (1996)
9. E. Alessio, A. Carbone, G. Castelli, and V. Frappietro "Second-order moving average and scaling of stochastic time series", Eur. Phys. Jour. B **27**, 197 (2002).
10. A. Carbone and G. Castelli, "Scaling properties of long-range correlated noisy signals: application to financial markets",in *Noise in Complex Systems and Stochastic Dynamics*, edited by L. Schimansky-Geier, D. Abbott, A. Neiman, and C. Van den Broeck, Proc. of SPIE **5114** (2003) 406.
11. A. Carbone, G. Castelli, and H. E. Stanley, "Analysis of clusters formed by the moving average of a long-range correlated time series", Phys. Rev. E **69** (2004) 026105.
12. Y. Ashkenazy, M. Lewkowicz, J. Levitan, S. Havlin, K. Saermark, H. Moelgaard, P.E.B. Thomsen, "Discrimination between healthy and sick cardiac autonomic nervous system by detrended heart rate variability analysis", Fractals **7**, 85 (1999)
13. G. Rangarajan and M. Ding, "Integrated approach to the assessment of long range correlation in time series data", Phys. Rev. E **61** 004991 (2000).
14. N. Vandewalle and M. Ausloos, "Crossing of two mobile averages: A method for measuring the roughness exponent", Phys. Rev. E, **58**, Issue 5 pp. 6832-6834, (1998)
15. Kun Hu, Plamen Ch. Ivanov, Zhi Chen, Pedro Carpena, and H. Eugene Stanley, "Effect of trends on detrended fluctuation analysis", Phys. Rev. E **64**, 011114, (2001)
16. Z. Chen, P. Ch. Ivanov, K. Hu, and H. E. Stanley, "Effect of Nonstationarities on Detrended Fluctuation Analysis," Phys. Rev. E **65** (2002) 041107.
17. C. Heneghan and G. McDarby, "Coherence and stochastic resonance in a two-state system", Phys. Rev. E, **62**, Issue 5, pp. 6103-6110 (2000)
18. J.S.Leu and A.Papamarcou, "On estimating the spectral exponent of fractional Brownian motion", IEEE Trans.Inf.Theory **41**, 233 (1995)
19. S.Thurner, M.C.Feurstein, and M.C.Teich "Multiresolution Wavelet Analysis of Heartbeat Intervals Discriminates Healthy Patients from Those with Cardiac Pathology" Phys. Rev. Lett. **80** (1998) 1544.
20. S.B.Lowen and M.C.Teich,"Fractal renewal processes generate 1/f noise",Phys. Rev.E **47** (1993) 992
21. M.C.Teich, C.Heneghan, S.B. Lowen, and R.G. Turcott"*Wavelets in Medicine and in Biology*", edited by A.Aldroubi and M.Unser (CRC Press, Boca Raton, FL, (1996))
22. Michel M. Dacorogna, Ramazan Genay, Ulrich Mller, Richard B. Olsen, Olivier V. Pictet, "*An Introduction to High-Frequency Finance*", Academic Press, (2001)
23. R.N. Mantegna and H.E. Stanley, "*An Introduction to Econophysics: Correlations and Complexity in Finance*", Cambridge University Press, 2000
24. R. F. Engle, "Autoregressive Conditional Heteroskedaticity with Estimates of the Variance of United Kingdom Inflation", Econometrica **50** (1982) 987.
25. T. Bollerslev, T. "Generalized Autoregressive Conditional Heteroskedasticity", J. Econometrics **31** (1986) 307.
26. R. F. Engle, "New Frontiers for ARCH Models", J. Appl. Econometrics **17** (2002) 425.

27. R. T. Baillie, T. Bollerslev, and H. O. Mikkelsen, "Fractionally Integrated Generalized Autoregressive Conditional Heteroskedasticity", J. Econometrics **74** (1996) 3.
28. R. N. Mantegna and H. E. Stanley, "Scaling Behaviour in the Dynamics of an Economic Index", Nature **376** (1996) 46.
29. X. Gabaix, P. Gopikrishnan, V. Plerou, and H. E. Stanley, "A Theory of Power-Law Distributions in Financial Market Fluctuations",Nature **423** (2003) 267.
30. B. B. Mandelbrot, A. Fisher, and L. Calvet, "A Multifractal Model of Asset Returns," [mimeo] Cowles Foundation for Research in Economics (1997).
31. L. Calvet and A. Fisher, "Multifractality in Asset Returns: Theory and Evidence," Rev. Econ. Stat. **84** (2002) 381–406.
32. T. Lux, "Turbulence in Financial Markets: The Surprising Explanatory Power of Simple Cascade Models," Quantitative Finance **1** (2001) 632–640.
33. E. F. Fama and K. R. French, "Permanent and Temporary Components of Stock Prices", J. Political Economy **96** (1988) 246.
34. J. Y. Campbell, "A Variance Decomposition of the Stock Returns", Econ. J. **101** (1991) 157.
35. J. Y. Campbell, "Why Long Horizons? A Study of Power against Persistent Alternatives", J. Empirical Finance **8** (2001) 459.
36. R. Priestly, "Time-Varying Persistence in Expected Returns", J. Banking and Finance, **101** (2001) 157.
37. U. Frisch and G. Parisi, G. in *Turbulence and Predictability in Geophysical Fluid Dynamics*, edited by M.Ghil (Kluwer North-Holland, Amsterdam, 1985), pp. 84–88.
38. A. Carbone, G. Castelli, and H. E. Stanley, "Time-Dependent Hurst Exponent in Financial Time Series", Physica A, in press, (2004) .
39. A. Arneodo, E. Bacry, and J. F. Muzy, "The Thermodynanics of Fractals Revisited with Wavelets," Physica A **213** (1993) 232–275.
40. G. C. Papanicolaou and K. E. Sølna, "Wavelet Based Estimation of Local Kolmogorov Turbulence," in *Theory and Applications of Long-Range Dependence*, edited by P. Doukham, G. Oppenheim and M. S. Taqqu (Birkhauser, Berlin, 2003), p. 473.
41. S. W. Smith, "Digital Filters," in *Digital Signal Processing: A Practical Guide for Engineers and Scientists* (Elsevier Science, Burlington MA, 2003), pp. 261–343.
42. R. H. Voss, "Random Fractal Forgeries," in NATO ASI series, Vol. F17 *Fundamental Algorithm for Computer Graphics*, edited by R. A. Earnshaw (Springer-Verlag, Berlin/Heidelberg, 1985).
43. O. Biham, Z.-F. Huang, O. Malcai, S. Solomon, "Long-time fluctuations in a dynamical model of stock market indices", Phys. Rev. E, **64**, 026101, (2001).
44. J. D. Hamilton, "State-Space Models", in *Handbook of Econometrics, Vol. IV*, edited by R. F. Engle and D. L. McFadden (Elsevier, Amsterdam, 1995), p. 3039.
45. K. Ivanova, M. Ausloos, "Low order variability diagrams for short range correlation evidence in financial data: BGL-USD exchange rate, Dow-Jones Industrial Average, Gold ounce price", Physica A, **265**, pp. 279-291 (1999)
46. P. Grau-Carles, "Long-range power-law correlations in stock returns", Physica A, **299**, 521, (2001).
47. P. Bak, C. Tang, and K. Wiesenfeld, "Self-organized criticality: An explanation of the 1/f noise", Phys. Rev. Lett. **59** (1987) 381.
48. P. Bak, C. Tang, and K. Wiesenfeld, "Self-organized criticality", Phys. Rev. A **38** (1988) 364.
49. C. Tang, K. Wiesenfeld, P. Bak, S. Coppersmith, and P. Littlewood, "Phase organization", Phys. Rev. Lett. 58, 1161-1164 (1987)
50. H. J. Jensen, *Self-Organized Criticality: Emergent Complex Behavior in Physical and Biological Systems* (Cambridge Univ. Press, Cambridge, 2000).
51. L. P. Kadanoff, S. R. Nagel, L. Wu, and S. Zhou, "Scaling and universality in avalanches", Phys. Rev. A **39** (1989) 6524.
52. Y. C. Zhang, "Scaling theory of self-organized criticality", Phys. Rev. Lett. **63** (1989) 470.
53. D. Dhar and R. Ramaswamy, "Exactly solved model of self-organized critical phenomena", Phys. Rev. Lett. **63** (1989) 1659.

54. D. Dhar, "Self-Organized Critical State of Sandpile Automation Models", Phys. Rev. Lett. **64** (1990) 1613.
55. K. Sneppen," Self-organized pinning and interface growth in a random medium", Phys. Rev. Lett. **69** (1992) 3539.
56. P. Bak and K. Sneppen, "Punctuated equilibrium and criticality in a simple model of evolution", Phys. Rev. Lett. **71** (1993) 4083.
57. K. Christensen, Z. Olami, and P. Bak, "Deterministic 1/f noise in nonconserative models of self-organized criticality", Phys. Rev. Lett. **68** (1992) 2417.
58. D.L.Turcotte, "Self-organized criticality", Rep. Prog. Phys. 62 (1999) 1377.
59. S. Maslov, M. Paczuski, and P. Bak, "Avalanches and 1 / f Noise in Evolution and Growth Models", Phys. Rev. Lett. **73** (1994) 2162.
60. M. Paczuski, S. Maslov, and P. Bak, "Avalanche dynamics in evolution, growth, and depinning models", Phys. Rev. E **53** (1996) 414.
61. S. S. Manna,"Two state model of self-organized criticality", J. Phys. A: Math. Gen. **24** (1991) L363.
62. B. Tadic, and D. Dhar,"Emergent Spatial Structures in Critical Sandpiles", Phys. Rev. Lett. **79** (1997) 1519.
63. M. Paczuski and K. E. Bassler, " Theoretical results for sandpile models of self-organized criticality with multiple topplings", Phys. Rev. E **62** (2000) 5347.
64. R. Pastor-Satorras and A. Vespignani, "Critical behavior and conservation in directed sandpiles", Phys. Rev. E **62** (2000) 6195.
65. D. Dhar,"Some results and a conjecture for Manna's stochastic sandpile model", Physica A **270** (1999) 69.
66. A. Chessa, H. E. Stanley, A. Vespignani, and S. Zapperi, "Universality in sandpiles" Phys. Rev. E **59** (1999) R12.
67. A. Vespignani, R. Dickman, M. A. Munoz, and S. Zapperi, "Absorbing-state phase transitions in fixed-energy sandpiles", Phys. Rev. E **62** (2000) 4564.
68. R. Dogaru *Universality and Emergent Computation in Cellular Neural Networks* (World Scientific Series in Nonlinear science, Singapore, 2003).
69. J.P. Boon Ed. *Lattice gas automata: Theory, simulation, implementation* J. Stat. Phys. **68** (1992).
70. J. R. Weimar and J.-P. Boon, "Class of cellular automata for reaction-diffusion systems", Phys. Rev. E **49**, 1749 (1994).
71. E. Domany and W. Kinzel, "Directed Percolation in Two Dimensions: Numerical Analysis and an Exact Solution", Phys. Rev. Lett. **47** (1981) 5.
72. E. Domany and W. Kinzel, "Equivalence of Cellular Automata to Ising Models and Directed Percolation", Phys. Rev. Lett. **53** (1984) 311.
73. F.Y. Wu and H.E.Stanley, "Domany-Kinzel Model of Directed Percolation: Formulation as a Random-Walk Problem and Some Exact Results", Phys. Rev. Lett. **48** (1982) 775.
74. A. Carbone and H. E. Stanley, "Directed Self-Organized Critical Patterns Emerging from Fractional Brownian Paths", Physica A, (2004), in press